

Evaluation of Mass Flux Representations of Vertical Velocity Fluctuations in Continental Stratus Clouds Using a mm-Wavelength Doppler Radar

*P. Kollias and B. A. Albrecht
University of Miami
Miami, Florida*

Introduction

A cloud mass flux representation of the vertical turbulent fluxes provides a physical framework for understanding the effects of shallow convection in maintaining the vertical structure of the boundary layer. This approach is based on the assumption that coherent updrafts and downdraft structures are responsible for most of the turbulent transport. Previous evaluations of mass flux parameterizations have been based on aircraft observations (e.g., Penc and Albrecht 1987) and results from Large Eddy Simulations (LESs) (e.g., Siebesma and Cuijpers 1995). In this study, mm-wavelength radar observations of vertical velocities in a continental stratus cloud are used to evaluate assumptions in the mass flux representations of the vertical-velocity variance. As part of this evaluation, direct sampling and conditional sampling techniques are used to define updraft and downdraft structures.

Data and Methodology

The observations used in this study were made in a continental stratus cloud observed over central Pennsylvania on November 18, 1995, from 0800 Universal Time Coordinates (UTC) to 1600 UTC. A series of 1-hour time-height cross sections of cloud reflectivity and vertical velocities at 2-second sampling intervals from a 94-GHz cloud radar provided a detailed mapping of the vertical cloud structure. Observations were made at night until late morning, covering a time period where the major source of buoyant energy for generating turbulence is longwave radiative cooling at cloud top. For the statistical analyses made in this study, velocity deviations from successive one-hour mean profiles of the vertical velocity were calculated. The removal of the mean aids in the identification of updraft and downdraft structures, filters out mesoscale vertical-velocity variability, and removes a mean velocity increase in the lower levels due to large-droplets at these levels. The temporal and vertical distribution of the velocity perturbations are in Figure 1 for the period 0900 UTC to 1000 UTC (0400 LST to 0500 LST). The boundary layer is fully coupled during this period. Later in the observing period there are clear signs of decoupling. A complete analysis of the decoupled period has also been made to allow for comparison with the coupled case. In this paper, however, we will only show the results for the coupled conditions. A comparison of these two time periods indicates a gradual shift of the updraft-downdraft activity from the upper part to the lower part of the cloud. During the later daytime period the updrafts and downdrafts are less intense and have less vertical extent.

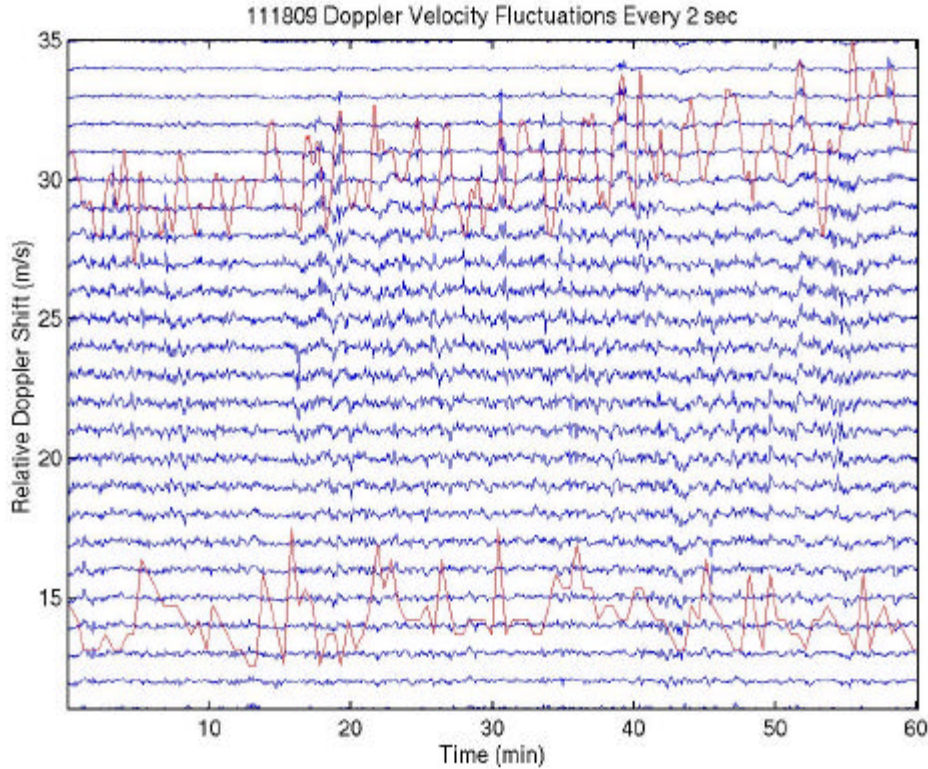


Figure 1. Time height mapping of the vertical velocity fluctuations, where the cloud boundaries are also shown.

A method proposed by Randall et al. (1992) (hereafter R92) for the determination of σ , the area covered by updrafts, and M_C , the mass flux, is applied to the observed velocity fluctuations. For this evaluation, two conditional sampling methods were applied to the data set. The first is a direct sampling scheme that is based only on the sign of the vertical velocity and the second adds a constraint on the vertical coherency of the structure to define updrafts and downdrafts. This constraint is that the sign of the vertical velocity is the same over a minimum vertical extent of 112 m (4 gates). The first sampling technique is the classical plume decomposition of the flow and the second is a coherent decomposition. More restricted flow decomposition techniques were also applied using a vertical velocity threshold. The above mentioned sampling techniques were applied and the updraft and downdraft subsets identified were used to evaluate the contribution of the top-hat and sub-plume variance to the vertical velocity variance (Wang and Stevens 1999). The decomposition of the variance into these two terms is given by:

$$\langle w'^2 \rangle = \sum_{i=1}^N \alpha_i w_i - \bar{w}^2 + \sum_{i=1}^N \alpha_i \langle w_i'^2 \rangle_i$$

where $i = 1 \dots N$ is the number of subsets (updrafts-downdrafts) that the vertical velocity time series is divided into and α_i is the fractional area occupied by an updraft/downdraft segment. The first term is the top-hat contribution to the variance and the second term is the sub-plume contribution. Such

decomposition is useful in evaluating the performance of the parameterization. If a high percentage of the observed variance is explained by the first term, then the parameterization is useful. Previous evaluations have been made using LES output, since the identification of vertically coherent structures is difficult to obtain with aircraft penetrations.

Results

The vertical profiles of average updraft and downdraft velocities (w_u and w_d) were estimated from the profiles of the statistical moments of the vertical velocity field by the method described by R92 for the 0900 UTC to 1000 UTC observing period. These values were compared with w_u and w_d by direct sampling of the w using the vertical velocity as an indicator (Figure 2). The profiles from the two techniques are similar, but as found by R92 using LES w fields, the statistical method overestimates the magnitude of the average upward and downward profiles. The magnitude and the vertical distribution are also very close to the LES derived results shown in R92. The vertical profiles of the fractional area α and mass-flux M_c corresponding to the one hour of analysis are shown in Figure 3. The estimates of M_c from the statistical method exceed those obtained by direct sampling and again the profiles have the

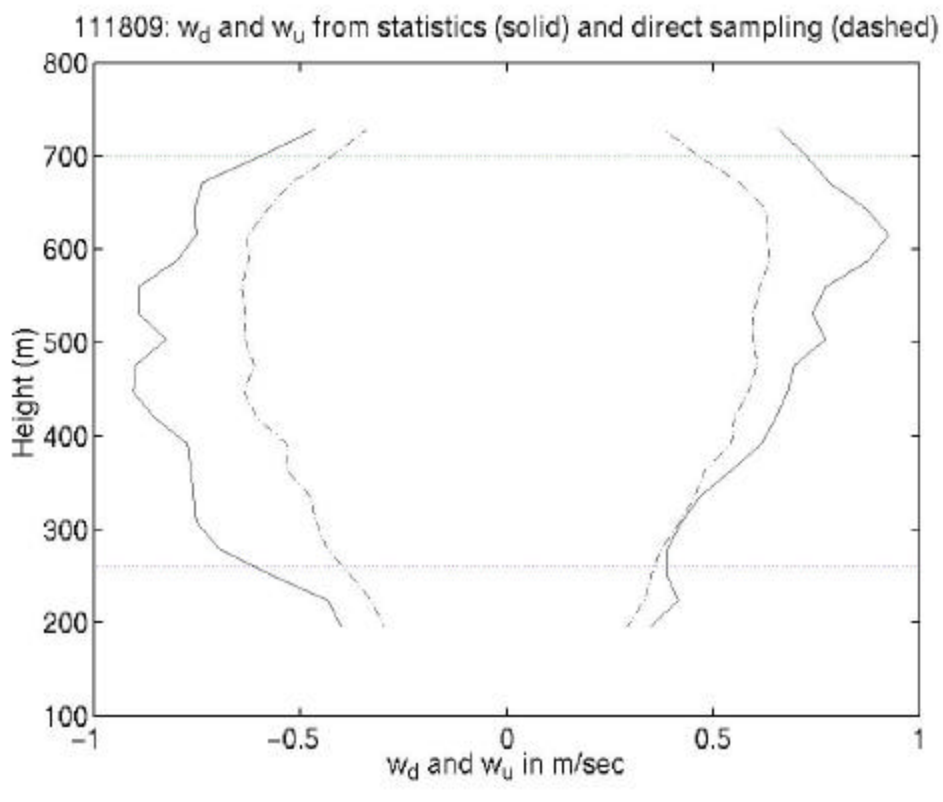


Figure 2. Vertical profiles of w_u and w_d calculated from direct sampling (dashed line) and from R92 method (solid line). Mean cloud base and cloud top are also shown.

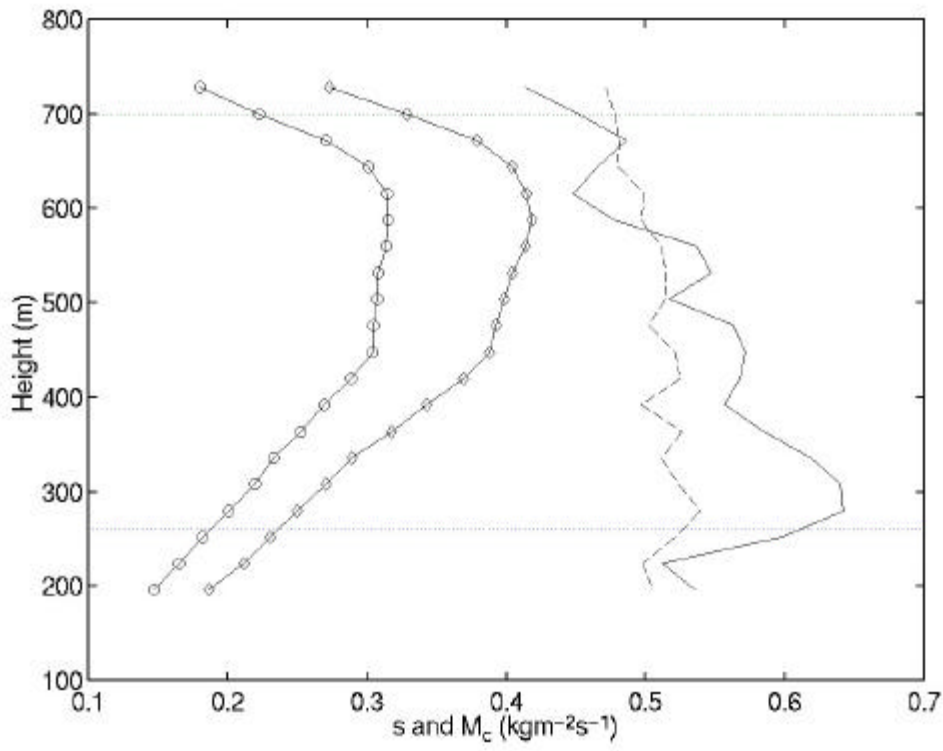


Figure 3. Vertical profiles of area of updrafts (dashed lines) and mass flux (circles) calculated from direct sampling (dashed line) and from R92 method (solid line and diamonds) for the coupled case. Mean cloud base and cloud top are also shown.

same behavior in the vertical as shown in R92 using LES results. Analyses of all eight 1-hour segments show similar results. The mass flux shown in Figure 3 has a maximum of $0.3 \text{ kgm}^{-2}\text{s}^{-1}$ in the upper part of the cloud layer where the maximum variance is observed. The fractional area covered by updrafts is close to 0.5, which is consistent with previous observations of stratocumulus. The area is slightly above 0.5 near the cloud base and below 0.5 near the cloud top. The fractional cloudiness calculated using the moments exaggerates the vertical variation of the fractional cloudiness. This case is offered for direct comparison with results from the third-order statistics produced by LES, since one of the ambiguities with the third-order statistics produced by LES models is the positive skewness in the upper part of the planetary boundary layer (PBL).

The contributions of updrafts of varying intensity to the mass flux were estimated using coherent sampling with different threshold limits (Figure 4). Updrafts with velocities less than 0.3 m/s are responsible for about half of the variance. The peak in the w variance near the upper portion of the cloud during this observational period reflects a strong peak in the updraft velocities at this level. In the decoupled case observed later in the period, there are two peaks in the mass flux profile. One peak is located in the upper part of the boundary layer while the other is located lower in the boundary layer.

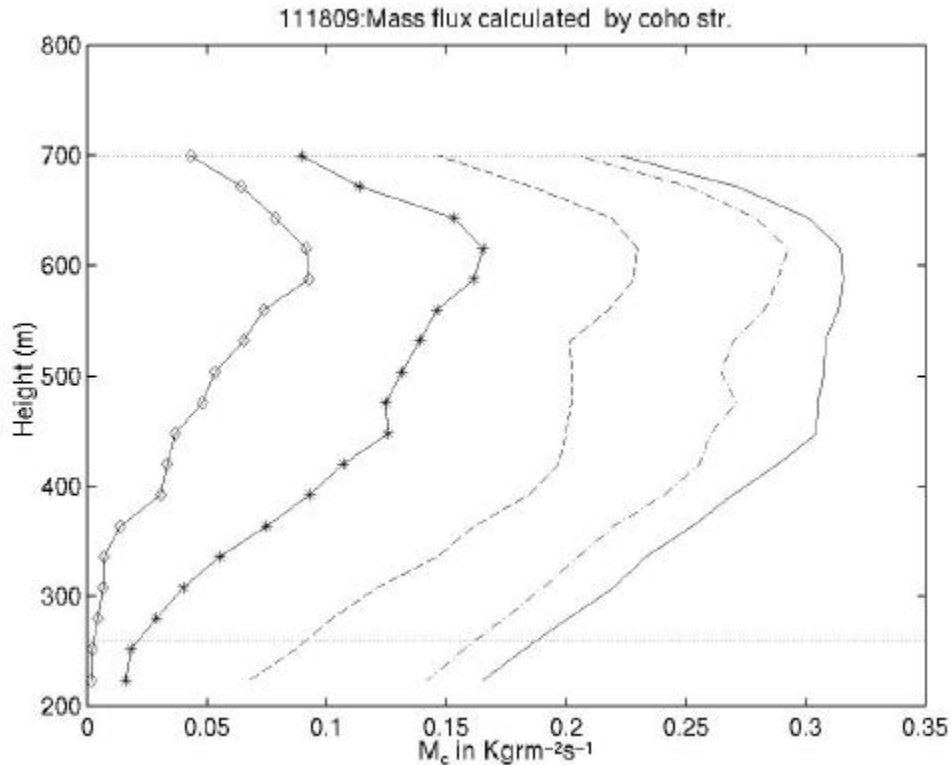


Figure 4. Mass-flux profiles calculated using coherent structure sampling techniques with different positive velocity thresholding (solid line is direct sampling, dot-dashed line coherent sampling with 0 m/sec threshold, dashed line coherent sampling with 0.3 m/sec threshold, solid line with stars coherent sampling with 0.6 m/sec threshold and solid line with diamonds coherent sampling with 1 m/sec threshold) for 0900 UTC to 1000 UTC.

The contributions of updrafts and downdrafts to the variance were further examined using the decomposition described by Wang and Stephens (1999). The vertical velocity variance profile during the coupled period (0900 UTC to 1000 UTC) and also the vertical profiles of the two terms (top-hat term and sub-plume term) are shown in Figure 5a. More than 70% of the variance is explained by the top-hat term, although that percentage varies slightly with height. In Figure 5b, the contributions of the updrafts and downdrafts are compared. The contributions are similar, but an interesting transition occurs above the location of the maximum variance. Below the variance maximum the downdraft contribution (both resolved and subplume) is higher than the contribution of the updrafts. Above the level of maximum variance the updraft contribution is higher. The upper cloud layer also has positive skewness, therefore the few narrow and intense updrafts have high “internal” (sub-plume) variability.

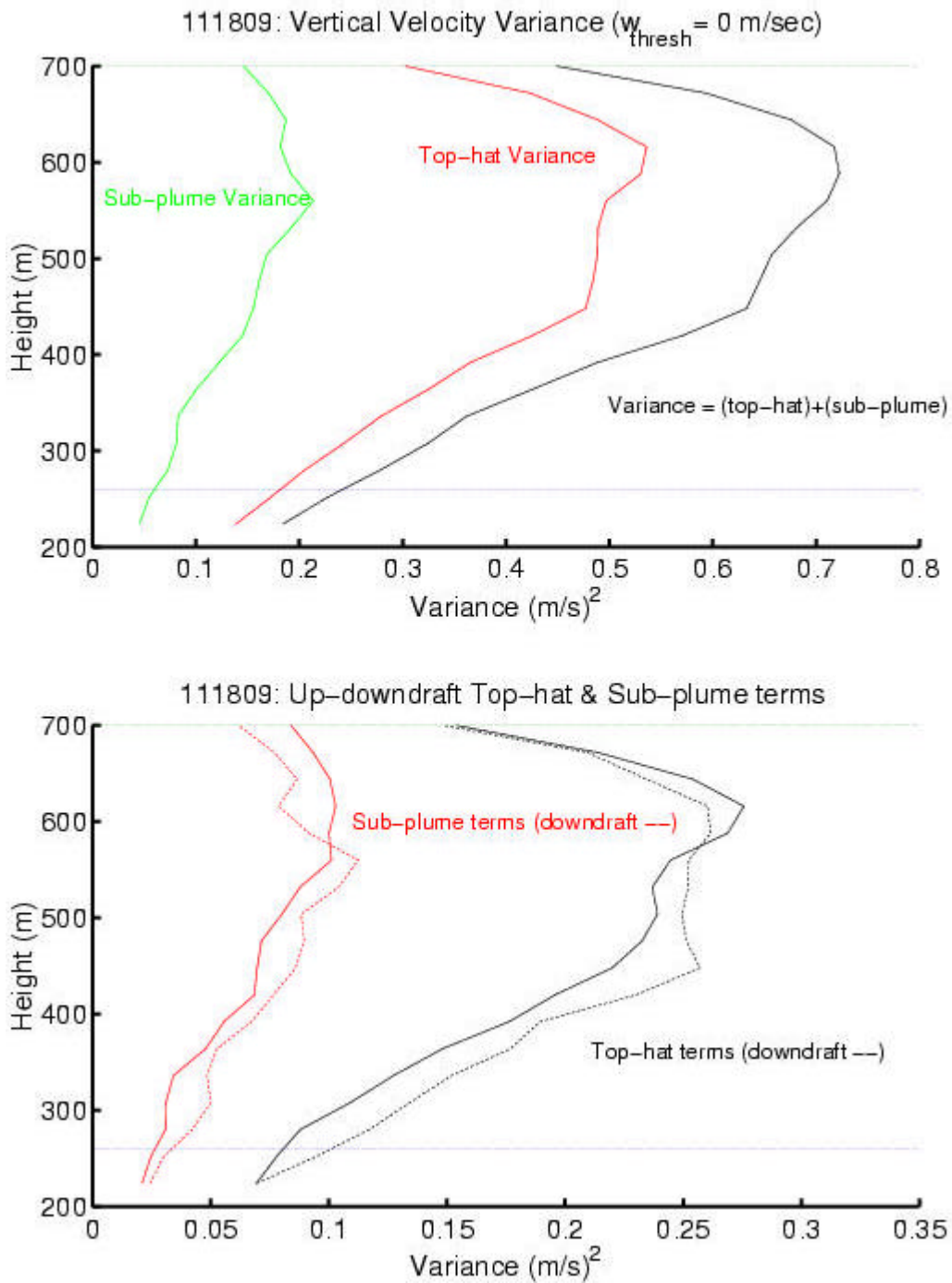


Figure 5. a) Vertical profile of the contribution of the top-hat and sub-plume term to the total variance for the couple case; b) decomposition of each term in updrafts and downdrafts.

Discussion

This radar study of continental stratocumulus provides a detailed comparison of the vertical velocity statistics and macroscopic cloud properties for coupled and decoupled boundary layer conditions during an 8-hour observing period. The vertically pointing mm-wavelength radar provides a detailed description of the turbulent cloud structure. The relatively uniform cloud boundaries and the nighttime character of the observations provide a unique case study of buoyancy driven cloud-topped boundary layer. This case is offered for direct comparison with the third-order statistics produced by LES. As higher processing rates become available on the Atmospheric Radiation Measurement (ARM) millimeter-wavelength radars, it will be possible to do similar analyses using observations from ARM.

References

- Penc, R. S., and B. A. Albrecht, 1987: Parametric representation of heat and moisture fluxes in cloud-topped layers. *Bound. Layer Meteor.*, **38**, 225-248.
- Randall, D. A., Q. Shao, and C.-H. Moeng, 1992: A second order bulk boundary-layer model. *J. Atmos. Sci.*, **49**(20), 1903-1923.
- Siebesma, A. P., and J. W. M. Cuijpers, 1995: Evaluation of parametric assumptions for shallow cumulus convection. *J. Atmos. Sci.*, **52**(6), 650-666.
- Wang, S., and B. Stevens, 1999: On top-hat representation of turbulence statistics in cloud-topped boundary layers: A large-eddy simulation study. *J. Atmos. Sci.* In press.